Loss of a Rho-Regulated Actin Nucleator, mDia2, Impairs Cytokinesis during Mouse Fetal Erythropoiesis

Sadanori Watanabe,[1,3] Tihana De Zan,[1,2,4] Toshimasa Ishizaki,[1,8] Shingo Yasuda,[1] Hiroshi Kamijo,[1] Daisuke Yamada,[1] Tomohiro Aoki,[1] Hiroshi Kiyonari,[5] Hiroshi Kaneko,[6] Ritsuko Shimizu,[6] Masayuki Yamamoto,[7] Gohta Goshima,[3] and Shuh Narumiya[1,2,*]

[1]Department of Pharmacology, Kyoto University Faculty of Medicine, Kyoto 606-8501, Japan
[2]Medical Innovation Center, Kyoto University Faculty of Medicine, Kyoto 606-8501, Japan
[3]Division of Biological Science, Graduate School of Science, Nagoya University, Nagoya 464-8602, Japan
[4]Division of Molecular Biology, Ruđer Bošković Institute, 10000 Zagreb, Croatia
[5]Laboratory for Animal Resources and Genetic Engineering, RIKEN Center for Developmental Biology, Kobe 650-0047, Japan
[6]Department of Molecular Hematology, Tohoku University Graduate School of Medicine, Sendai 980-8575, Japan
[7]Department of Medical Biochemistry, Tohoku University Graduate School of Medicine, Sendai 980-8575, Japan
[8]Present address: Department of Pharmacology, Oita University Faculty of Medicine, Oita 879-5593, Japan
*Correspondence: snaru@mfour.med.kyoto-u.ac.jp
http://dx.doi.org/10.1016/j.celrep.2013.10.021

SUMMARY

The small GTPase Rho and mDia2, a Rho-regulated actin nucleator, function as critical regulators of cytokinesis in cultured cells. However, their involvement in cytokinesis during mammalian development remains unknown. Here, we generated mice deficient in mDia2 and examined the role of Rho signaling in cytokinesis during development. mDia2-deficient mice survive until embryonic day 11.5 (E11.5), exhibit severe anemia with multinucleate erythroblasts, and die in utero by E12.5. mDia2-deficient erythroid cells differentiate normally, though in a delayed manner, but exhibit cytokinesis failure with decreased accumulation of F-actin in the cleavage furrow during late differentiation from proerythroblasts. On the other hand, inactivation of Rho induces cytokinesis failure from the earlier progenitor stage. mDia2-deficient erythroblasts, however, are able to enucleate their nuclei. Our findings have thus revealed that mDia2 functions critically in cytokinesis in vivo during erythropoiesis and further suggest that the cytokinesis mechanism in development diverges downstream of Rho. They also demonstrate that cytokinesis and enucleation utilize different mechanisms.
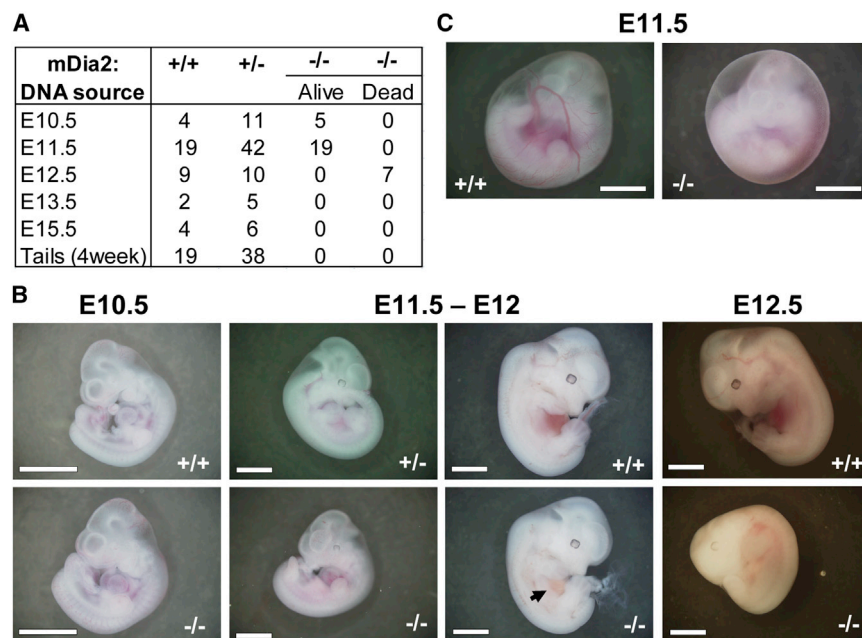
INTRODUCTION

In animal cytokinesis, actin filaments accumulate around the equator of a dividing cell in anaphase to form a ring-like apparatus, called the contractile ring, and myosin-based contraction of this ring physically separates a dividing cell into two in telo-phase (Green et al., 2012; Pollard, 2010). The small GTPase Rho functions as a molecular switch of cytokinesis by recruiting actin nucleators and preparing the contractile apparatus at the site of contraction (Jordan and Canman, 2012). Two types of actin filaments, branched and unbranched, are formed in cells through the action of actin nucleators, typically the Arp2/3 complex and the formin family proteins, respectively (Firat-Karalar and Welch, 2011). Involvement of Rho and the Rho-regulated formin family proteins in cytokinesis is conserved during evolution, Rho1p and Bnil1p in budding yeasts, Rho-1 and Cyk-1 in worms, and Rho1 and Diaphanous in flies (Balasubramanian et al., 2004). In mammalian cells, Rho acts on the mDia family of formin proteins for de novo formation of actin filaments (Narumiya and Yasuda, 2006). There are three isoforms of mDia: mDia1–mDia3 (Alberts et al., 1998; Watanabe et al., 1997; Yasuda et al., 2004). Although depletion of mDia1 and/or mDia3 does not interfere with cytokinesis, cytokinesis failure occurs on depletion of mDia2 in cultured cells (Watanabe et al., 2008), suggesting that the Rho-mDia2 signaling operates as a mechanism of cytokinesis in mammalian cells. However, such analysis has been limited to cultured cells, and the role of Rho-mDia pathway in cytokinesis in vivo remains to be determined. We recently generated mice deficient in mDia1 or mDia3 or both and found that these knockout (KO) mice develop to adulthood (Sakata et al., 2007; Shinohara et al., 2012), further indicating the importance of mDia2 for cytokinesis in vivo. We have now generated mice deficient in mDia2 and examined its role in cytokinesis during development.

RESULTS

Loss of mDia2 Leads to Embryonic Lethality

To investigate in vivo functions of mDia2, we disrupted the murine mDia2 gene (Figures S1A–S1D). Whereas mDia2 hetero-zygous-deficient (mDia2^{+/−}) mice were born healthy and fertile

A

mDia2: DNA source	+/+	+/−	−/− Alive	−/− Dead
E10.5	4	11	5	0
E11.5	19	42	19	0
E12.5	9	10	0	7
E13.5	2	5	0	0
E15.5	4	6	0	0
Tails (4week)	19	38	0	0

C E11.5

B

E10.5   E11.5 – E12   E12.5

Figure 1. Loss of mDia2 Leads to Embryonic Lethality

(A) Genotype analysis shows progeny from mDia2$^{−/−}$ intercross.

(B) Representative photographs show mDia2$^{+/+}$, mDia2$^{+/−}$, and mDia2$^{−/−}$ embryos at various developmental stages. Note that the fetal liver of an mDia2$^{−/−}$ embryo at E12 is anemic (indicated by an arrow). Scale bars, 2 mm.

(C) Representative photographs show mDia2$^{+/+}$ and mDia2$^{−/−}$ yolk sacs at E11.5. Note that the yolk sac of an mDia2$^{−/−}$ embryo contains less blood. Scale bars, 2 mm.

See also Figure S1.

without any noticeable phenotype, all homozygous-deficient (mDia2$^{−/−}$) mice from mDia2$^{+/−}$ intercrosses died in utero (Figure 1A), indicating that mDia2 is essential for embryonic development. Because mDia2 is essential for cytokinesis in cultured cells (Watanabe et al., 2008), we suspected that mDia2$^{−/−}$ embryos die at an early developmental stage due to cytokinesis failure. However, we found that mDia2$^{−/−}$ embryos survived without severe malformations in their body until embryonic day 10.5 (E10.5) after gestation (Figures 1B and S1E) and died in utero around E12.5 (Figure 1A). mDia2$^{−/−}$ embryos were found viable at the expected Mendelian ratio at E11.5 but paler and smaller than their wild-type littermates (Figures 1A and 1B). Although the heart functioned normally, and the blood vessels in the yolk sacs were formed normally in mDia2$^{−/−}$ embryos (Movies S1 and S2; Figure S1E), their yolk sacs appeared to have a less amount of blood than that of wild-type (Figure 1C), suggesting the presence of anemia in mDia2$^{−/−}$ embryos.

### mDia2 Is Required for Fetal Erythropoiesis

In mouse embryos, primitive erythropoiesis, which is characterized by the production of nucleated erythrocytes, is initiated in blood islands of the yolk sac at E7.5 (Palis et al., 2010). Although peripheral blood at E11.5 contains mostly nucleated primitive erythroblasts (Fraser et al., 2007), analysis of peripheral blood in E11.5 mDia2$^{−/−}$ embryos revealed that their circulating blood cells were less in number than wild-type littermates, large, and frequently binuclear or multinuclear (Figures 2A–2C, S2A, and S2B), suggesting the primitive erythropoiesis failure in mDia2$^{−/−}$ embryos. In addition to this primitive erythropoiesis, the definitive erythropoiesis starts around E11.5 in the fetal liver, in which a massive number of enucleated erythrocytes are produced from erythroblasts (Baron et al., 2012). Hematopoietic stem cells in fetal livers continuously replenish erythroid progenitors for the production of erythrocytes during late gestation. We therefore

hypothesized that mDia2 is involved also in erythropoiesis in the fetal liver. Erythroid progenitors and erythroblasts in fetal liver can be distinguished by examining surface markers such as CD71 and Ter119 (Zhang et al., 2003) (Figures S2C and S2D). Flow cytometry of wild-type and mDia2$^{−/−}$ fetal liver cells at E11.5 showed that mDia2$^{−/−}$ fetal liver contained a significantly less number of Ter119^{+} erythrocytes and lower percentage of Ter119^{+}/CD71^{+} cells than wild-type control: 10.5% ± 5.5% (n = 4) and 22.5% ± 4.0% (n = 5) (p = 0.015), respectively (Figures S2E, 2D, and 2E). Probably reflecting this reduction of the erythroblast population, the percentages of Ter119$^{−}$/CD71^{+} erythroid populations were higher in the mDia2$^{−/−}$ fetal liver than the wild-type control (Figure 2D). These results together suggest that mDia2 is required for both primitive and definitive erythropoiesis.

mDia2 Is Required for Expansion of Differentiating Erythroblasts

The above results suggest that mDia2 plays critical roles in production of erythroid cells. To clarify at which step mDia2 regulates erythropoiesis, we first examined burst-forming unit erythroids (BFU-Es) and more mature erythroid colony-forming unit erythroids (CFU-Es) in the fetal liver at E11.5. Both types of colonies were formed even in the absence of mDia2. However, the colony numbers of BFU-Es and CFU-Es were significantly lower in mDia2$^{−/−}$ cells than those of mDia2$^{+/−}$ cells (Figure 3A), and CFU-E colony formation was more severely reduced in mDia2$^{−/−}$ cells. These results suggest that mDia2 regulates erythropoiesis preferentially downstream of CFU-E (Figure S2C). We next used an in vitro culture system for erythroid cell differentiation (Zhang et al., 2003) to examine erythropoiesis failure in mDia2$^{−/−}$ cells in more detail. Ter119$^{−}$ cells were purified from fetal livers and cultured in the presence of erythropoietin (EPO). In this system, proliferation and differentiation of erythroid cells were examined by counting the cell number, Wright-Giemsa staining, and flow cytometry analysis. Counting the viable cell number revealed that proliferation was severely impaired in mDia2$^{−/−}$ fetal liver cells compared to the mDia2$^{+/−}$ cells (Figure 3B); the increase of the cell number was delayed already at 12 hr and significantly suppressed at 24 and 36 hr.
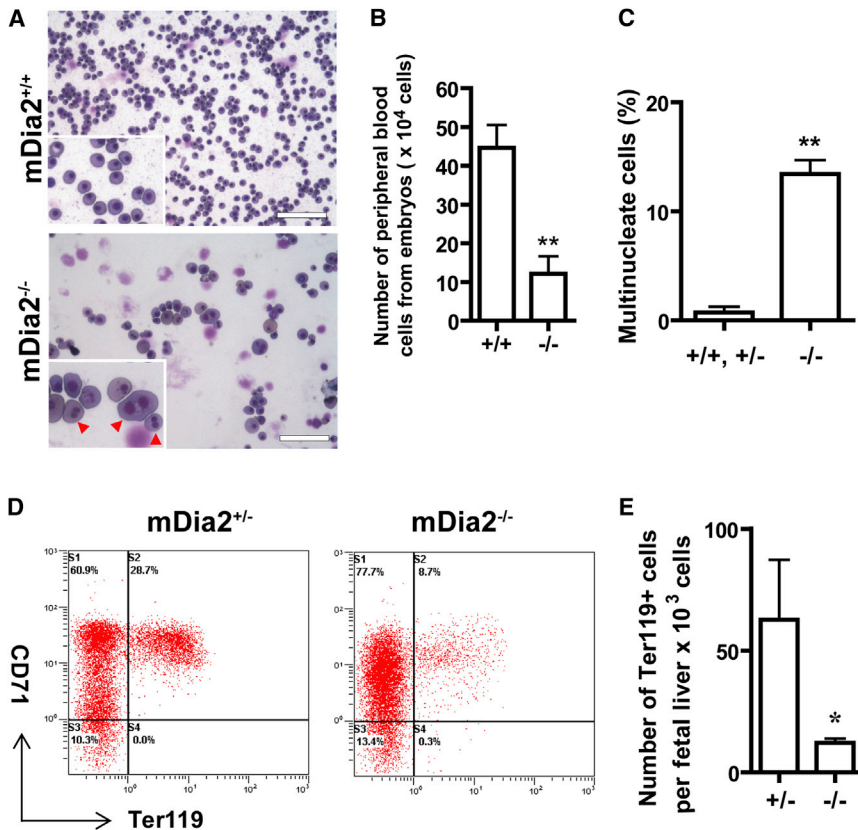
Figure 2. Impaired Erythropoiesis of mDia2 KO Embryo

(A) Wright-Giemsa staining of peripheral blood from mDia2$^{+/+}$ and mDia2$^{-/-}$ embryos. Arrowheads show multinucleate erythroblasts. Scale bars, 0.1 mm.

(B) Number of erythroblasts in total peripheral blood from mDia2$^{+/+}$ (n = 10) and mDia2$^{-/-}$ (n = 7) embryos at E11.5 is shown. Data are represented as mean ± SEM. **p < 0.01 (Mann-Whitney U test).

(C) Percentages of multinucleate erythroblasts in peripheral blood from mDia2$^{+/+}$ or mDia2$^{+/-}$ and mDia2$^{-/-}$ embryos at E11.5 are presented. The graph shows the mean ± SD of five independent experiments, in each of which >200 cells were examined. **p < 0.01 (Mann-Whitney U test).

(D) Flow cytometry shows fetal liver cells from mDia2$^{+/+}$ and mDia2$^{-/-}$ embryos at E11.5. Propidium iodide (PI)-positive dead cells were excluded from the analysis. The representative of more than three experiments is shown.

(E) Number of Ter119$^+$ cells in fetal livers of mDia2$^{+/-}$ (n = 6) and mDia2$^{-/-}$ (n = 8) embryos at E11.5 is shown. Data are represented as mean ± SEM. *p < 0.05 (Mann-Whitney U test).

See also Figure S2.

were observed often in multinucleate erythroblasts (Figure S3D).

To further identify the differentiation step at which mDia2 deficiency impairs proliferation and induces apoptosis, we subjected cells of 0, 12, 24, and 36 hr of culture to flow cytometry analysis. In control mDia2$^{+/-}$ cells, more than 90% of the population was CD71^{high} Ter119$^-$ at 12 hr of culture (Figure 3F), among which most appeared as c-Kit$^-$ (Figure S3E), indicating that they represent proerythroblasts (Dev et al., 2010). mDia2$^{+/-}$ cells were then enriched in the Ter119$^+$CD71$^+$ c-Kit$^-$ population in a time-dependent manner at 24 and 36 hr, indicating that they differentiated to polychromatic or orthochromatic erythroblasts (Figures 3F and S3E) (Zhang et al., 2003). On the contrary, although mDia2$^{-/-}$ cells were enriched in the CD71^{high} Ter119$^-$ population at 12 hr, there was a significantly less accumulation of these cells in the Ter119$^+$CD71$^+$ population at 24 and 36 hr (Figure 3F). Because the appearance of apoptotic cells was associated with multinucleation and decreased viable cell number in mDia2$^{-/-}$ cells, a smaller accumulation of this genotype of cells in the polychromatic or orthochromatic erythroblast population suggests that multinucleation either in the transition from proerythroblast or during terminal differentiation induces apoptosis in these populations.

To examine whether the loss of mDia2 affects expression of erythroid differentiation characteristics in this process, we analyzed expression of several erythroid-related genes. We found no significant difference between mDia2$^{+/+}$ or mDia2$^{+/-}$ and mDia2$^{-/-}$ cells in expression of *Slc4a1*, *Spna1*, *EpoR*, and *Gata1* at 12 and 24 hr (Figure S3F). Interestingly, *mDia2* expression increased during in vitro differentiation of erythroblasts, as reported previously by Ji et al. (2008); its expression more than
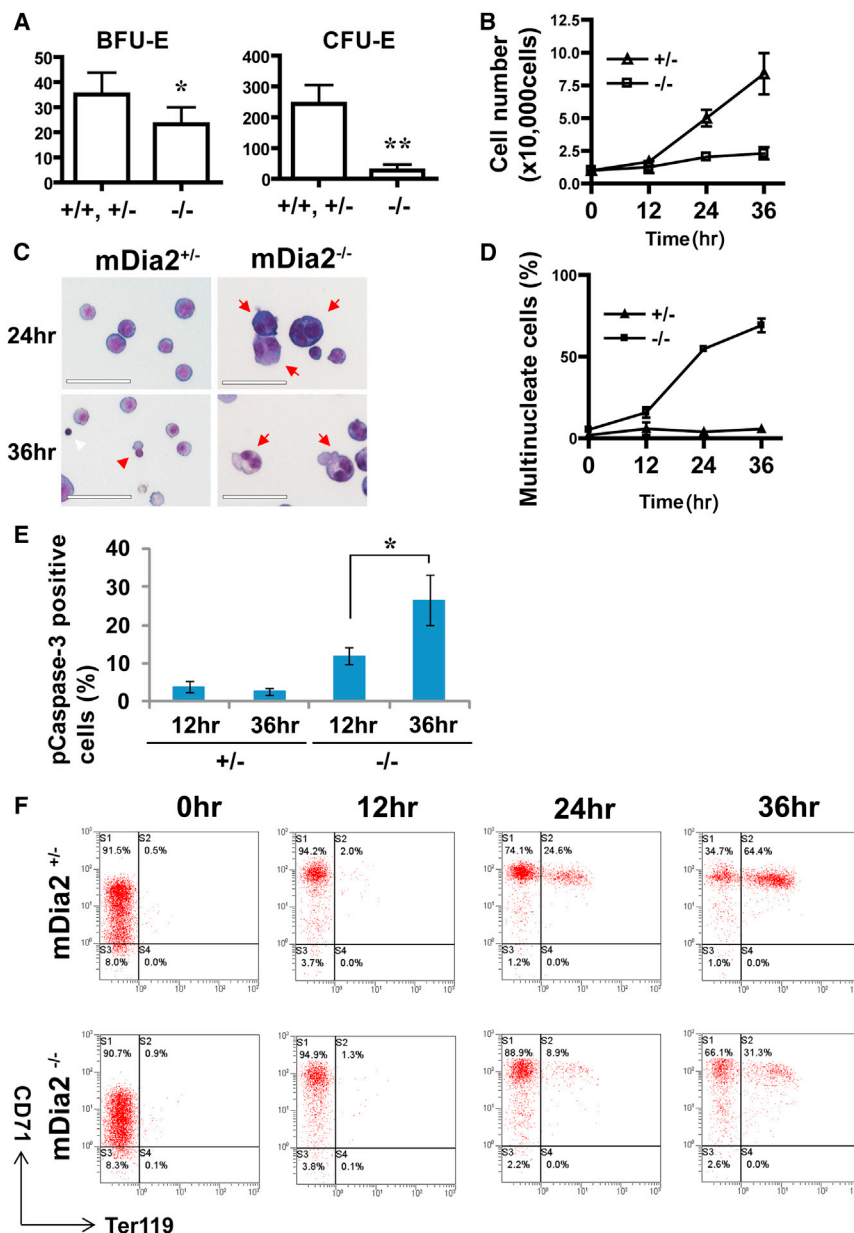
Concomitant with this suppression of cell proliferation, multinucleate cells increased in number in mDia2$^{-/-}$ cells from 12 to 36 hr of culture (Figures 3B–3D), suggesting that the proliferation defect was coupled with cytokinesis failure in mDia2$^{-/-}$ cells. We next treated the Ter119$^-$ mDia2$^{+/-}$ cells with cytochalasin D for 12 hr and found that a much higher population of cells (more than 80% of the cytochalasin D-treated cells) became multinucleated at 12 hr (Figure S3A) than mDia2$^{-/-}$ cells (15.8% ± 3.1%) (Figure 3D). These findings demonstrate that cytokinesis occurs in the earlier stage of erythroid differentiation through control of F-actin assembly and that the cytokinesis at this stage is carried out without involvement of mDia2. We therefore next wondered whether an upstream molecule, Rho, is involved in the cytokinesis of the early stage of differentiation by introducing a Rho-specific inhibitor, C3, into the cells. Notably, 70% of the C3-treated cells became multinucleated at 12 hr (Figure S3B). These results suggest that Rho controls cytokinesis from the earlier differentiation stage, whereas its effector, mDia2, becomes important for cytokinesis in the later stages of erythroid differentiation. We then used mDia2 siRNA. Depletion of mDia2 induced multinucleation of cultured cells, and Giemsa staining suggested that they were late-stage erythroblasts (Figure S3C), confirming the cytokinesis failure in mDia2$^{-/-}$ cells. Notably, the number of activated caspase-3$^+$ cells increased time dependently in the mDia2$^{-/-}$ cell population (Figure 3E), suggesting that decreased proliferation and increased multinucleate cell number are associated with apoptotic cell death. Indeed, signals of activated caspase-3

Figure 3. Impaired Proliferation and Multinucleation of mDia2 KO Erythroblasts during Erythroid Differentiation In Vitro

(A) Quantification of BFU-Es and CFU-Es in the fetal liver of mDia2$^{+/+}$ or mDia2$^{+/-}$ and mDia2$^{-/-}$ embryos. Colony assays were carried out with 5,000 cells prepared from the fetal liver of indicated genotypes at E11.5. Data are mean ± SD from five (BFU-Es) and three (CFU-Es) mice in each group. **p < 0.01 and *p < 0.05 (Welch test).

(B–F) Erythroid differentiation of mDia2$^{-/-}$ fetal liver cells in vitro is shown. Ter119^{-} erythroid progenitor cells were purified from the fetal liver of E11.5 mDia2$^{+/-}$ or mDia2$^{-/-}$ embryos and cultured in medium containing EPO. Aliquots were taken at 0, 12, 24, and 36 hr and subjected to analysis.

(B) Cell proliferation during in vitro erythroid differentiation is shown. Data are mean ± SD from three independent experiments.

(C) Wright-Giemsa staining of mDia2$^{+/-}$ or mDia2$^{-/-}$ erythroblasts at 24 and 36 hr culture. Red arrows show multinucleate cells. Red and white arrowheads show enucleating cells and enucleated nuclei, respectively. Scale bars, 50 μm.

(D) Percentages of multinucleate cells during erythroid differentiation are presented. The graph shows the mean ± SD of three independent experiments, in each of which >200 cells were examined.

(E) Percentages of phosphorylated caspase-3 (pCaspase-3)-positive cells in mDia2$^{+/-}$ and mDia2$^{-/-}$ cells are shown. More than 200 cells from mDia2$^{+/-}$ (n = 3) or mDia2$^{-/-}$ (n = 4) embryos at E11.5 were analyzed, and the results are represented as mean ± SD. *p < 0.05 (Welch test).

(F) Flow cytometry shows mDia2$^{+/-}$ and mDia2$^{-/-}$ cells during erythroid differentiation. PI-positive dead cells were excluded from the analysis.

See also Figure S3.

tripled in 24 hr (Figure S3G). These results together suggest that the loss of mDia2 does not directly block differentiation of erythroblasts but affects proliferation of differentiating erythroblasts possibly through cytokinesis failure.

mDia2 Is Essential for Cytokinesis but Not for Enucleation of Erythroblasts

In the terminal stage of erythroid differentiation in mouse, one proerythroblast cell undergoes three cycles of mitosis with decreasing its cell size and sequentially generating basophilic, polychromatic, and orthochromatic erythroblasts, of which the latter finally expel their nuclei to produce reticulocytes (Hattangadi et al., 2011; Liu et al., 2013). To analyze how the loss of mDia2 affects terminal erythroid differentiation, we monitored

the process of cytokinesis during erythroid differentiation by live-cell imaging (Figure 4A). Cells from mDia2$^{+/+}$ as well as mDia2$^{+/-}$ fetal liver underwent rounds of successful cell divisions with decreasing their size (Figure 4A, top). On the other hand, mDia2$^{-/-}$ erythroblasts frequently failed in cytokinesis by exhibiting aberrant contraction (Figure 4A, bottom). The cleavage furrow was formed initially but got destabilized during contraction, and the ingression was then fused back, and the cell could not complete cytokinesis (Figure 4A). Notably, smaller mDia2$^{-/-}$ cells failed in cytokinesis more frequently than larger mDia2$^{-/-}$ cells; the percentage of cytokinesis failure in mDia2$^{-/-}$ cells was 84.8% (n = 33) and 18.2% (n = 33) in smaller (<12.5 μm) and larger cells (>12.5 μm), respectively. Given that erythroblasts decrease their size during differentiation, these results suggest that mDia2 plays an essential role in the cytokinesis of erythroblasts in the terminal stage of differentiation, i.e., of basophilic or polychromatic erythroblasts. Because mDia2 induces F-actin for the contractile ring in cultured mammalian cells (Watanabe et al., 2008), we stained for mDia2 and F-actin in differentiating
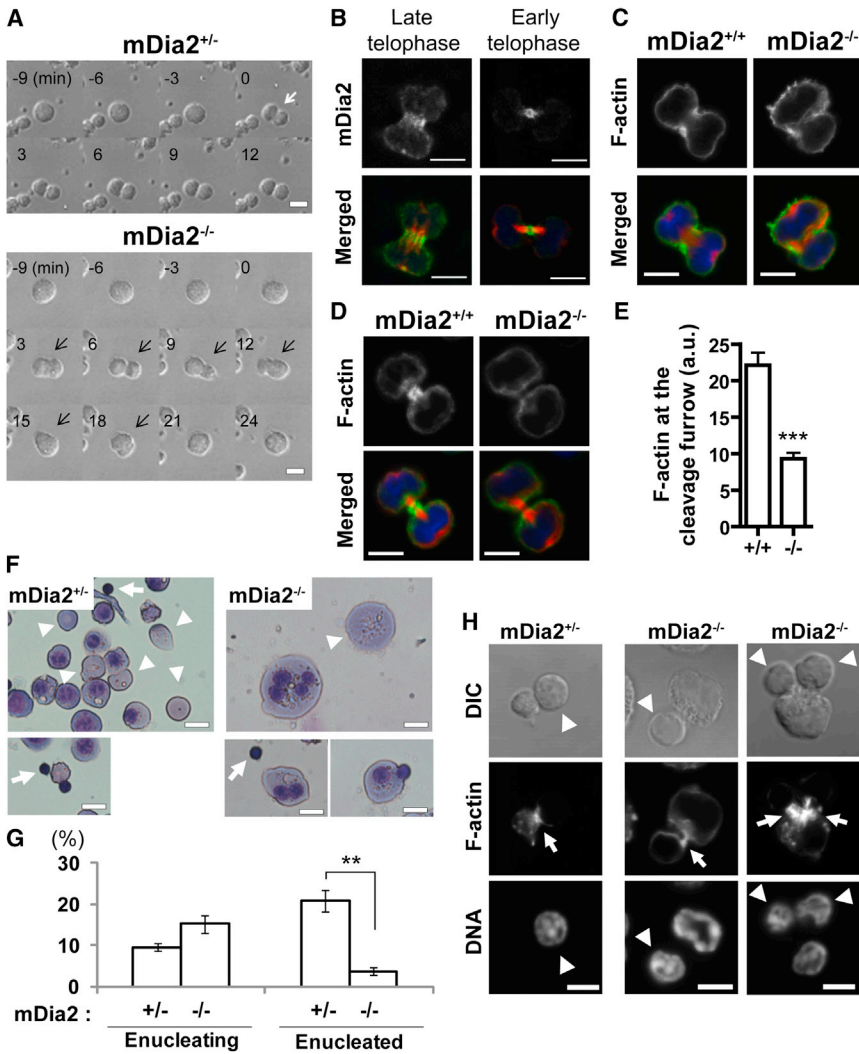
Figure 4. Analysis of Cytokinesis and Enucleation in mDia2 KO Erythroblasts

(A) Live imaging shows cell division of in-vitro-differentiated mDia2$^{+/-}$ (top) and mDia2$^{-/-}$ (bottom) erythroblasts. Fetal liver cells were isolated from embryos at E11.5 and cultured in medium containing EPO for 24 hr. Division of erythroblasts was then monitored every 3 min for 6 hr. Scale bars, 10 μm. White and black arrows show normal and abnormal contraction of erythroblasts, respectively.

(B) Localization of mDia2 in dividing wild-type erythroblasts is shown. Wild-type erythroblasts in cytokinesis at 24 hr culture were stained for mDia2 (green), α-tubulin (red), and DNA (blue). Examples of more than 20 cells are shown. Scale bars, 5 μm.

(C–E) Abnormal localization of F-actin (C) and impaired accumulation of F-actin at the cleavage furrow (D and E) and in mDia2$^{-/-}$ erythroblasts are shown. Dividing erythroblasts from mDia2$^{+/-}$ and mDia2$^{-/-}$ fetal liver were stained for F-actin (red), α-tubulin (green), and DNA (blue). Scale bars, 5 μm. In (E), fluorescence intensity at the cleavage furrow in erythroblasts of 20 cells in each group from two independent experiments was quantified as described in Experimental Procedures. Data are presented as mean ± SEM. ***p < 0.001 (Mann-Whitney U test).

(F–H) Analysis of enucleation in mDia2 KO erythroblasts is shown. Ter119$^-$ erythroid progenitor cells were isolated as described in Figure 3B and cultured for 24 hr in medium containing EPO. The cells were further cultured for another 16 hr (H) or 36 hr (F and G) in medium without EPO.

(F) Wright-Giemsa staining shows mDia2$^{+/-}$ and mDia2$^{-/-}$ erythroblasts. Small panels show examples of enucleating and enucleated erythroblasts, and arrows and arrowheads indicate ejected nuclei and enucleated cells, respectively. Scale bars, 20 μm.

(G) Frequency of enucleation in mDia2$^{-/-}$ erythroblasts is presented. The graph shows the mean ± SEM of three independent experiments, in each of which >200 orthochromatic erythroblasts were examined. **p < 0.05 (Welch test).

(H) Immunofluorescence shows enucleating erythroblasts from mDia2$^{+/-}$ and mDia2$^{-/-}$ embryos. Cells were stained for F-actin and DNA. Arrowheads and arrows indicate nuclei protruding from cells and accumulation of F-actin, respectively. Scale bars, 5 μm.

See also Figure S4.

erythroid cells. mDia2 signals were observed at the cleavage furrow (Figure 4B), where F-actin also localized, in wild-type cells. On the other hand, in mDia2$^{-/-}$ cells, F-actin accumulation was either seen at aberrant sites or was severely impaired at the cleavage furrow after ingression (Figures S4C–S4E). These results suggest that mDia2 is required for production of F-actin at the proper position of the cleavage furrow in erythroblasts to perform persistent contraction of the contractile ring during cytokinesis.

We next examined enucleation in mDia2$^{-/-}$ erythroblasts. Enucleation occurs in two steps: the first is protrusion of the nucleus, and the second is pinching off the protruded nucleus (Palis, 2012). We found that multinucleate mDia2$^{-/-}$ erythroblasts frequently showed protrusion of their nuclei (Figures 4F–4H and S4A; Movie S3). Consistent with the notion that the nuclear protrusion is carried out by the F-actin assembly, F-actin

accumulated at the boundary between the cytoplasm and the protruded nuclei in mDia2$^{-/-}$ erythroblasts as seen in mDia2 wild-type and mDia2$^{+/-}$ cells (Figure 4G). We then wondered if mDia2$^{-/-}$ multinucleate erythroblasts could complete enucleation and found that there are big enucleated mDia2$^{-/-}$ erythroblasts, though with reduced frequency compared to that of mDia2$^{+/-}$ erythroblasts (Figures 4F and 4G). These results suggest that mDia2 is not essential for the enucleation process at least in vitro. In addition to mDia2$^{-/-}$ cells, Rho-inactivated multinucleate erythroblasts also showed nuclear protrusion in enucleation (data not shown), suggesting that F-actin assembly pathways other than Rho-mDia2 function in enucleation. We therefore examined the effects of inhibitors of actin polymerization and other small GTPases regulating F-actin assembly (Ji et al., 2008; Konstantinidis et al., 2012; Wang et al., 2012). The protrusion of nuclei and F-actin accumulation in multinucleate

mDia2$^{-/-}$ cells were inhibited by treatment of the cells with cyto-chalasin D, latrunculin A, and a Rac1 inhibitor (Figures S4B–S4D; Movie S4). These results suggest that the Rac-dependent F-actin assembly pathway functions in erythroblasts and that Rho and mDia2 are dispensable in this process, indicating the cooperation of multiple Rho GTPase signaling pathways to ensure the successful production of erythrocytes (Ji et al., 2008) (Figure S4E).

DISCUSSION

Here, we have revealed the essential role of mDia2 for cytokinesis of erythroblasts during mouse development. Our main findings are discussed below.

First, our study demonstrated that the Rho-mDia2 signaling found in cultured cells (Watanabe et al., 2008) indeed functions in cytokinesis in vivo and plays an essential role in development. Our findings have thus revealed the involvement of an actin nucleator in mammalian somatic cytokinesis in vivo. Previous findings on the involvement of actin nucleators in cytokinesis were limited to meiosis (Leader et al., 2002; Pfender et al., 2011; Yi et al., 2011). Importantly, the cytokinesis failure phenotype of mDia2-deficient mice was most evident during erythropoiesis. Such erythropoiesis failure was not found in either mDia1-deficient (Peng et al., 2007; Sakata et al., 2007) or mDia3-deficient mice, although immunofluorescence signal for mDia1 is observed in the cleavage furrow and midbody of erythroblasts (S.W., unpublished data). These results indicate that mDia2 rather than mDia1 and mDia3 functions critically in erythroblast cytokinesis. Why the phenotype of mDia2-deficient mice, the cytokinesis failure, is mainly observed in erythropoiesis remains to be investigated. Because similar erythropoiesis-specific cytokinesis failure is observed in patients with congenital dyserythropoietic anemia, who have a mutation in KIF23 (Liljeholm et al., 2013), one of the important factors controlling RhoA in cytokinesis, these results might reflect the high susceptibility of erythroid cells to the defect in Rho signaling. We further identified the point of the mDia2 action in cytokinesis at the stage of basophilic and polychromatic erythroblasts. Because cell death is frequently observed in multinucleate erythroblasts, the proliferation defect is most probably due to the cytokinesis failure of erythroblasts, though we could not exclude additional mechanisms. The impaired cytokinesis during erythroid differentiation in mDia2$^{-/-}$ cells might also delay the differentiation of erythroblasts. These results taken together suggest that the cytokinesis failure in erythroblasts is the major cause of anemia in mDia2$^{-/-}$ mice, which finally results in the embryonic lethality in the mice.

Second, and equally importantly, we discovered that mDia2 is not always essential for cytokinesis. Indeed, mDia2$^{-/-}$ embryos developed until E11.5. We also found that cytokinesis of erythroid progenitors is not sensitive to the loss of mDia2 but fails upon Rho inactivation and treatment with actin polymerization inhibitors. It is noteworthy that the frequency of cytokinesis failure increased during erythroblast differentiation, and although the full ingression of cleavage furrow was often observed in mDia2$^{-/-}$ erythroblasts of a relatively bigger size

in the early stage, no or little ingression was observed in more differentiated, smaller erythroblasts. These results implicate an alternative actin nucleator or F-actin assembly pathway downstream of Rho during cytokinesis of erythroid progenitor cells and suggest that mDia2 replaces their role during erythroblast differentiation. It is interesting in this respect that expression of mDia2 more than tripled during this time.

Finally, we have revealed that cytokinesis and enucleation are driven by different Rho-GTPase signaling mechanisms. Previously, Ji et al. (2008) reported that the percentage of enucleated erythroblasts in mDia2 shRNA-treated cells was decreased and suggested the involvement of mDia2 in enucleation. We also found the similar decrease of the number of enucleated cells from mDia2$^{-/-}$ cells. However, we suggest that this is due to the cytokinesis failure during erythroid differentiation, which resulted in the decrease of orthochromatic erythroblasts and increase in multinucleated cells. The multinucleation itself might also affect the efficiency of enucleation due to the increase in the number of nuclei in one cell, although multinucleate mDia2$^{-/-}$ erythroblasts could extrude their nuclei with F-actin accumulation, albeit lower frequency, to give rise to big enucleated cells. On the other hand, the nuclear protrusion in mDia2$^{-/-}$ erythroblasts was blocked by inhibition of Rac or F-actin depolymerization, which is in accordance with the previous reports by Ji et al. (2008) and Konstantinidis et al. (2012). These results suggest the presence of other uncharacterized F-actin assembly mechanisms downstream of Rac in the enucleation process.

In summary, we have identified the Rho-mDia2 pathway as the conserved Rho-formin family protein axis in cytokinesis of erythroblasts in vivo. Our study has further demonstrated that mDia2 is not critical in cytokinesis of every type of cell and that Rac utilizes yet unidentified actin-dependent mechanisms in enucleation.

EXPERIMENTAL PROCEDURES

Hematological Analysis and In Vitro Differentiation of Erythroid Cells

We have obtained all the necessary permissions from boards of animal and DNA experiments in Kyoto University and RIKEN CDB for the mice used in our research. Fetal livers were isolated from E11.5–E12 embryos and mechanically dissociated by pipetting with a 25G needle in Iscove's Modified Dulbecco's Medium (IMDM) containing 2% FBS (STEMCELL Technologies). Single-cell suspensions were prepared by passing the dissociated cells through a 25 μm cell strainer (BD Falcon). In vitro erythroid differentiation was performed according to Zhang et al. (2003). In brief, fetal liver cells were labeled with biotin-conjugated Ter119 antibody (BD Pharmingen), and Ter119$^-$ cells were purified through MS column and Streptavidin MicroBeads (Miltenyi Biotec). Purified cells were seeded with IMDM GlutaMAX (Invitrogen), 15% FBS (STEMCELL Technologies), 200 μg/ml holo-transferrin, 10 μg/ml recombinant human insulin, 0.1 mM β-mercaptoethanol (Invitrogen), 1× penicillin-streptomycin mixed solution (PS) (Nacalai Tesque), and 2 U/ml EPO (Roche) into a dish precoated with 50 μg/ml fibronectin (Sigma-Aldrich). The cells were maintained at 37°C with an atmosphere containing 5% CO_2. For Figures 4F–4H and S4, the medium was replaced at 24 hr culture with IMDM GlutaMAX containing 20% FBS, 1× PS, and 0.1 mM β-mercaptoethanol and further cultured for 12–36 hr.

Statistical Analysis

Data are presented as mean ± SD or SEM and were evaluated using indicated statistical tests on Prism 4.0 software (GraphPad). A value of p < 0.05 was considered statistically significant.

REFERENCES

Alberts, A.S., Bouquin, N., Johnston, L.H., and Treisman, R. (1998). Analysis of RhoA-binding proteins reveals an interaction domain conserved in heterotrimeric G protein beta subunits and the yeast response regulator protein Skn7. J. Biol. Chem. 273, 8616–8622.

Balasubramanian, M.K., Bi, E., and Glotzer, M. (2004). Comparative analysis of cytokinesis in budding yeast, fission yeast and animal cells. Curr. Biol. 14, R806–R818.

Baron, M.H., Isern, J., and Fraser, S.T. (2012). The embryonic origins of erythropoiesis in mammals. Blood 119, 4828–4837.

Dev, A., Fang, J., Sathyanarayana, P., Pradeep, A., Emerson, C., and Wojchowski, D.M. (2010). During EPO or anemia challenge, erythroid progenitor cells transit through a selectively expandable proerythroblast pool. Blood 116, 5334–5346.

Firat-Karalar, E.N., and Welch, M.D. (2011). New mechanisms and functions of actin nucleation. Curr. Opin. Cell Biol. 23, 4–13.

Fraser, S.T., Isern, J., and Baron, M.H. (2007). Maturation and enucleation of primitive erythroblasts during mouse embryogenesis is accompanied by changes in cell-surface antigen expression. Blood 109, 343–352.

Green, R.A., Paluch, E., and Oegema, K. (2012). Cytokinesis in animal cells. Annu. Rev. Cell Dev. Biol. 28, 29–58.

Hattangadi, S.M., Wong, P., Zhang, L., Flygare, J., and Lodish, H.F. (2011). From stem cell to red cell: regulation of erythropoiesis at multiple levels by multiple proteins, RNAs, and chromatin modifications. Blood 118, 6258–6268.

Ji, P., Jayapal, S.R., and Lodish, H.F. (2008). Enucleation of cultured mouse fetal erythroblasts requires Rac GTPases and mDia2. Nat. Cell Biol. 10, 314–321.

Jordan, S.N., and Canman, J.C. (2012). Rho GTPases in animal cell cytokinesis: an occupation by the one percent. Cytoskeleton (Hoboken) 69, 919–930.

Konstantinidis, D.G., Pushkaran, S., Johnson, J.F., Cancelas, J.A., Manganaris, S., Harris, C.E., Williams, D.A., Zheng, Y., and Kalfa, T.A. (2012). Signaling and cytoskeletal requirements in erythroblast enucleation. Blood 119, 6118–6127.

Leader, B., Lim, H., Carabatsos, M.J., Harrington, A., Ecsedy, J., Pellman, D., Maas, R., and Leder, P. (2002). Formin-2, polyploidy, hypofertility and positioning of the meiotic spindle in mouse oocytes. Nat. Cell Biol. 4, 921–928.

Liljeholm, M., Irvine, A.F., Vikberg, A.L., Norberg, A., Month, S., Sandström, H., Wahlin, A., Mishima, M., and Golovleva, I. (2013). Congenital dyserythropoietic anemia type III (CDA III) is caused by a mutation in kinesin family member, KIF23. Blood 121, 4791–4799.

Liu, J., Zhang, J., Ginzburg, Y., Li, H., Xue, F., De Franceschi, L., Chasis, J.A., Mohandas, N., and An, X. (2013). Quantitative analysis of murine terminal erythroid differentiation in vivo: novel method to study normal and disordered erythropoiesis. Blood 121, e43–e49.

Narumiya, S., and Yasuda, S. (2006). Rho GTPases in animal cell mitosis. Curr. Opin. Cell Biol. 18, 199–205.

Palis, J. (2012). Losing a "nucleus" to gain a cytoplasm. Blood 119, 5948–5949.

Palis, J., Malik, J., McGrath, K.E., and Kingsley, P.D. (2010). Primitive erythropoiesis in the mammalian embryo. Int. J. Dev. Biol. 54, 1011–1018.

Peng, J., Kitchen, S.M., West, R.A., Sigler, R., Eisenmann, K.M., and Alberts, A.S. (2007). Myeloproliferative defects following targeting of the Drf1 gene encoding the mammalian diaphanous related formin mDia1. Cancer Res. 67, 7565–7571.

Pfender, S., Kuznetsov, V., Pleiser, S., Kerkhoff, E., and Schuh, M. (2011). Spire-type actin nucleators cooperate with Formin-2 to drive asymmetric oocyte division. Curr. Biol. 21, 955–960.

Pollard, T.D. (2010). Mechanics of cytokinesis in eukaryotes. Curr. Opin. Cell Biol. 22, 50–56.

Sakata, D., Taniguchi, H., Yasuda, S., Adachi-Morishima, A., Hamazaki, Y., Nakayama, R., Miki, T., Minato, N., and Narumiya, S. (2007). Impaired T lymphocyte trafficking in mice deficient in an actin-nucleating protein, mDia1. J. Exp. Med. 204, 2031–2038.

Shinohara, R., Thumkeo, D., Kamijo, H., Kaneko, N., Sawamoto, K., Watanabe, K., Takebayashi, H., Kiyonari, H., Ishizaki, T., Furuyashiki, T., et al. (2012). A role for mDia, a Rho-regulated actin nucleator, in tangential migration of interneuron precursors. Nat Neurosci 15, 373–380, S371–S372.

Wang, J., Ramirez, T., Ji, P., Jayapal, S.R., Lodish, H.F., and Murata-Hori, M. (2012). Mammalian erythroblast enucleation requires PI3K-dependent cell polarization. J. Cell Sci. 125, 340–349.

Watanabe, N., Madaule, P., Reid, T., Ishizaki, T., Watanabe, G., Kakizuka, A., Saito, Y., Nakao, K., Jockusch, B.M., and Narumiya, S. (1997). p140mDia, a mammalian homolog of Drosophila diaphanous, is a target protein for Rho small GTPase and is a ligand for profilin. EMBO J. 16, 3044–3056.

Watanabe, S., Ando, Y., Yasuda, S., Hosoya, H., Watanabe, N., Ishizaki, T., and Narumiya, S. (2008). mDia2 induces the actin scaffold for the contractile ring and stabilizes its position during cytokinesis in NIH 3T3 cells. Mol. Biol. Cell 19, 2328–2338.

Yasuda, S., Oceguera-Yanez, F., Kato, T., Okamoto, M., Yonemura, S., Terada, Y., Ishizaki, T., and Narumiya, S. (2004). Cdc42 and mDia3 regulate microtubule attachment to kinetochores. Nature 428, 767–771.

Yi, K., Unruh, J.R., Deng, M., Slaughter, B.D., Rubinstein, B., and Li, R. (2011). Dynamic maintenance of asymmetric meiotic spindle position through Arp2/3-complex-driven cytoplasmic streaming in mouse oocytes. Nat. Cell Biol. 13, 1252–1258.

Zhang, J., Socolovsky, M., Gross, A.W., and Lodish, H.F. (2003). Role of Ras signaling in erythroid differentiation of mouse fetal liver cells: functional analysis by a flow cytometry-based novel culture system. Blood 102, 3938–3946.